APL Submission.
JAN 2003.

2565

NSOM analysis of standing waves in fiber Bragg gratings

J.C. Gates, J.D. Mills, and W.S. Brocklesby

Optoelectronics Research Centre,

University of Southampton

Highfield,

Southampton SO17 1BJ U.K.

Abstract

NSOM can provide direct information about the electric fields inside optoelectronic devices with sub-wavelength resolution. This paper describes the first direct measurements of the amplitude and phase of the standing waves within a fiber Bragg grating, using a heterodyne interference variant of NSOM working at telecommunications wavelengths. The amplitudes of forward and backward-going components of the standing wave can be measured separately, and the π phase shift between the standing wave nodes as the wavelength varies across the stop band is imaged directly for the first time in any photonic crystal structure.

Fiber Bragg gratings are one of the most important new components for telecommunications[1] since the EDFA. They also represent the most successful practical example of the use of photonic crystals, although only one-dimensional. Most of the analysis of the properties of gratings is based on examination of their reflection and transmission spectra. These measurements can provide a great deal of useful information, but necessarily always average across the whole grating. As grating manufacture techniques become more sophisticated, tremendous control can be exerted over the form of individual grating planes, allowing production of discrete phase slips[2], or superstructure. In order to study the local properties of the grating, it is necessary to use a technique which can resolve detail on the scale of the planes of the grating, usually ~500nm period. One optical technique with the required resolution is near-field scanning optical microscopy (NSOM), which can image the distribution of light within the grating by sampling the evanescent field tails of the fiber mode, if the grating is side-polished to within a few microns of the core. In previous work[3], photon scanning tunneling microscopy (PSTM) of the evanescent field has been used to image the intensities of standing waves within fiber Bragg gratings at 800nm. In this paper we demonstrate direct imaging of the amplitude and phase of the light within the grating across the wavelength range of usage in telecommunications. This allows measurement of the relative amplitudes of the forward and backward propagating waves within the grating, and the variation in position of the standing wave nodes relative to the grating as the wavelength of the light is tuned across the grating stop band.

NSOM detection of the evanescent field tails of the fiber mode is performed by removing a significant thickness of the fiber cladding by polishing, which in turn changes the form of the propagating modes. To minimise fiber mode changes, a few microns of cladding is left on the fiber, and a very sensitive detection technique is used to overcome the resultant small signal levels. The sensitivity is provided by an elegant heterodyne interferometric technique developed by van Hulst *et al*[4], which allows detection of the amplitude and phase of the optical signal directly as a function of tip position.

In the case of NSOM detection of a standing wave such as is found in a Bragg grating using a heterodyne interferometric technique, the output from the interferometer is a combination of three fields: the forward and backward travelling waves in the grating and the field from the reference arm. We can write the sum of the signal (E_s) and reference (E_r) fields as:

$$E_s + E_r = A_f e^{i(\omega t - kx)} + A_b e^{i(\omega t + kx + \gamma)} + A_r e^{i[(\omega + \omega_m)t + \beta]} \qquad (1)$$

where A_f, A_b are the amplitudes of the forward and backward-going waves inside the grating, A_r is the amplitude of the reference wave, ω is the light frequency, ω_m is the heterodyne frequency shift, β is a phase shift between signal and reference arms, and γ is a phase shift between the forward and backward-going waves. The component of the photodetector signal, $|E_s + E_r|^2$, at the modulation frequency ω_m can itself be resolved into two components, which can be recovered directly from the two phases of the lock-in amplifier. These two components are given by

$$\begin{aligned} V_{\cos} &\propto A_f \cos(\beta + kx) + A_b \cos(kx + \gamma - \beta) \\ V_{\sin} &\propto -A_f \sin(kx + \beta) + A_b \sin(kx + \gamma - \beta) \end{aligned} \qquad (2)$$

and correspond to the fields that make up the standing wave itself at a particular time, which is defined by the relative phase shift β. The detected values of A_f and A_b

include the effect on the mode-tip coupling of modes with different evanescent field extents; this makes quantitative comparisons for cladding modes more complex

The gratings used in this experiment were written using an excimer laser interferometer. The gratings were side-polished to expose evanescent fields to measure with the NSOM. Light from a tuneable diode laser was coupled into the polished grating, and collected using an uncoated fiber tip held 5-10nm from the sample surface using standard shear force techniques[5]. Polarization of the input light was controlled using an in-fiber polarizer. The light from the tip was combined with the frequency-shifted reference beam in a fiber coupler, and detected by an InGaAs diode. The whole experiment was carefully thermally isolated, in order to give a phase stability in the interferometer of 330 /hour. The grating stop bands for TE and TM-polarised light were not significantly shifted in frequency, demonstrating that the propagation constants for the two orthogonal polarizations were not significantly different despite the polishing. The polished surface of the grating was flat to within ±10nm within any given scan, removing the influence of topographical artefacts.

Figure 1(a) shows the transmission spectrum of the grating used in these experiments. Cross-sections of the amplitude and phase along the grating with the laser tuned to the wavelength marked W on the grating transmission curve are shown in figures 1(b) and 1(c). Only a small modulation is visible in the amplitude, as the grating reflectivity here is low. The variation of the optical phase along the waveguide is approximately what would be expected for a single propagating mode. We can model the variation of amplitude and phase with four parameters: an overall amplitude scaling parameter, the ratio of A_f/A_b, a phase angle, and the propagation constant for the mode in question. Fits to the amplitude and phase variation are shown in the figure – very good agreement with the model is found, with a value of A_f/A_b of 5.2. In this wavelength region the ratio of the forward and backward-going wave amplitudes, A_f/A_b, is expected to be large, as the grating reflects very little light.

Figure 2(a) shows a linear greyscale image of the amplitude of the evanescent field near the grating stop band, taken near the center of the 2cm-long grating. The image is divided into two halves. The lower half is taken with the laser tuned to the short-wavelength edge of the stop band (marked Y in figure 1), and the upper half is taken with the laser tuned to the long wavelength edge (marked Z). The image demonstrates the first physical measurement of the π phase change between the two, as predicted explicitly for fiber gratings[6] and in general for photonic band gap systems[7]. Figure 2(b) shows cross-sections of the image along the center of the grating at the two wavelengths used for the image in 2(a). Figure 2(c) shows a cross-section of the phase as a function of distance along the grating. At this wavelength where grating reflectivity is high, the ratio of the forward and backward-going amplitudes is close to one, producing the characteristic shape shown. This phase variation is fitted well by the model described earlier in the paper. Similar phase variation has previously been seen in simple standing wave patterns of evanescent waves within a prism[8].

As the probe laser wavelength is tuned through the different regions of grating reflectivity, different behaviour can be seen in the amplitude and phase variation. As the laser source is tuned through the stop band, A_f/A_b is almost unity, and the physical position of the nodes varies as detailed above. As the laser is tuned below the stop band, where cladding modes are excited in reflection rather than core modes, different behavior is seen. A_f/A_b is increased through the whole region, as the intensity in the backward-going wave decreases with decreasing grating reflectivity. At position X in the transmission pattern, where the lowest-order cladding mode is excited, clear interference is seen between the forward-going core mode and the backward going cladding mode, which results in the pattern shown in figure 3. The backward-going cladding mode is LP11, with each lobe having opposite E-field directions. This causes the interference to be alternately constructive and destructive for each lobe in antiphase along the grating, resulting in the alternating pattern shown in the figure.

In conclusion, we have demonstrated direct imaging of the amplitude and phase of the standing wave within a fiber Bragg grating at telecommunications wavelengths. Several features of the grating predicted by theory, such as the positions of the nodes at frequencies either side of the stop band, and the variation of the amplitude of the backward-going wave have been measured directly for the first time. Using this technique, together with D-fiber gratings with more well-defined mode structures, it will be possible to quantify many of the previously only theoretical results concerning the electric field variation within complex fiber gratings.

The authors would like to thank Professor Michael Zervas for helpful discussions.

Figure Captions

Figure1(a): transmission spectrum of fiber grating used for these experiments. (b) Standing wave amplitude versus distance along grating at wavelength W. Dots are data, solid line is theory described in text; (c) Phase of standing wave versus distance along grating at wavelength W – symbols as (b)

Figure 2(a): Image of standing wave intensity centered along length of grating. Top half of image is at wavelength Z (figure 1), on the long-wavelength edge of the grating stop band. Bottom half of image is taken at wavelength Y, on the short wavelength edge of the stop band. The π phase shift between the edges of the stop band is clearly visible from comparison of the two halves of the image. (b) Cross-section along fiber core axis of image in (a) at the two wavelengths shown. (c) Phase variation along grating at wavelength at wavelength Y, short-wavelength edge of stop band. Dots are data, solid line is predicted from theory described in text.

Figure 3: Image of standing wave intensity taken at wavelength X (figure 1), where the backward-going wave is a low-order (LP11) cladding mode, resulting in the interference shown in the figure.

Figure 1, J.C. Gates et al.

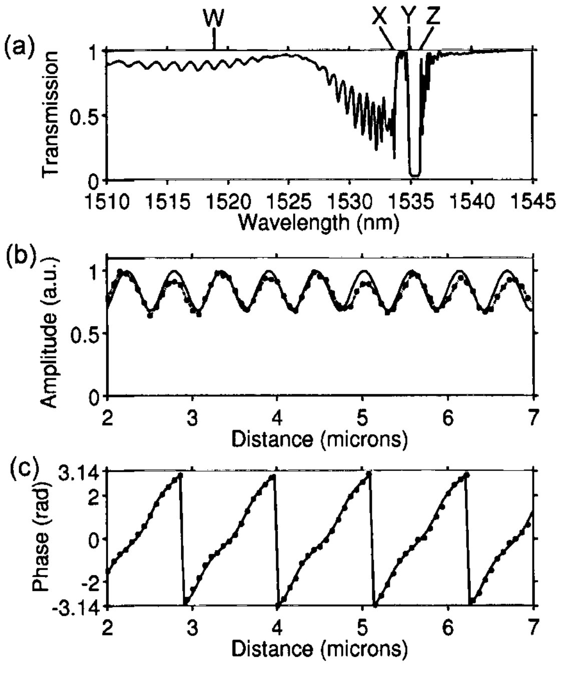

figure 2, J.C. Gates et al.

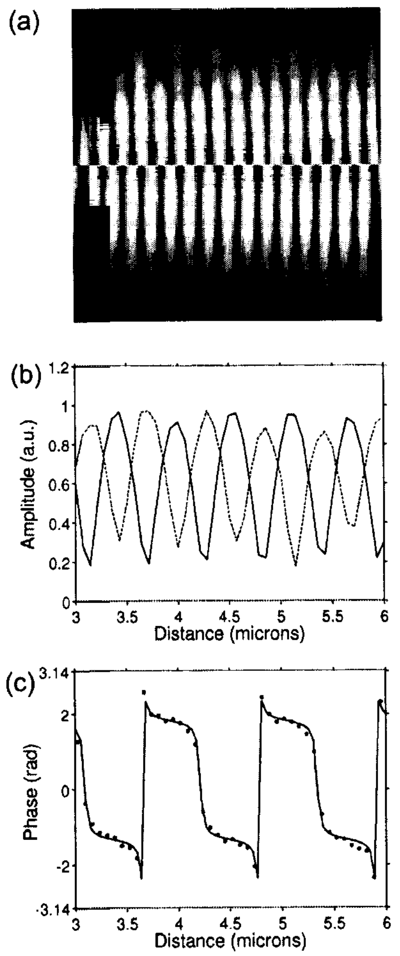

Figure 3, J.C. Gates et al.

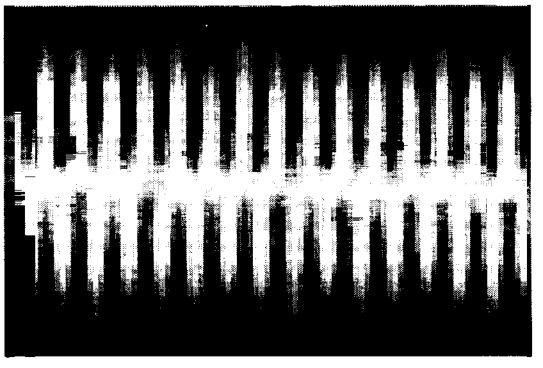

References

[1] R. Kashyap, *Fiber Bragg Gratings.* (Academic Press, 1999).

[2] A. Asseh, H. Storoy, J.T. Kringlebotn, W. Margulis, B. Sahlgren, S. Sandgren, R. Stubbe, and G. Edwall, Electronics Letters **31** (12), 969 (1995).

[3] J. D. Mills, C. W. J. Hillman, W. S. Brocklesby, and B. H. Blott, Applied Physics Letters **75** (26), 4058 (1999).

[4] M. L. M. Balistreri, J. P. Korterik, L. Kuipers, and N. F. van Hulst, Physical Review Letters **85** (2), 294 (2000).

[5] K. Karrai and R. D. Grober, Applied Physics Letters **66** (14), 1842 (1995).

[6] V. Finazzi and M.N. Zervas, Appl. Opt. **41** (12), 2240 (2002).

[7] J.D. Joannopoulos, R.D. Meade, and J.N. Winn, *Photonic Crystals: Molding the flow of Light*, 1st ed. (Princeton University Press, Princeton, 1995).

[8] A. Nesci, R. Dandliker, and H. P. Herzig, Optics Letters **26** (4), 208 (2001).